nature medicine

Caspase 3–mediated stimulation of tumor cell repopulation during cancer radiotherapy

Qian Huang[1–3,12], Fang Li[2,12], Xinjian Liu[2], Wenrong Li[2], Wei Shi[4], Fei-Fei Liu[4], Brian O'Sullivan[4], Zhimin He[2], Yuanlin Peng[5], Aik-Choon Tan[6], Ling Zhou[7], Jingping Shen[2], Gangwen Han[8], Xiao-Jing Wang[8–10], Jackie Thorburn[11], Andrew Thorburn[11], Antonio Jimeno[6,9,10], David Raben[2,9], Joel S Bedford[5] & Chuan-Yuan Li[2,10,11]

In cancer treatment, apoptosis is a well-recognized cell death mechanism through which cytotoxic agents kill tumor cells. Here we report that dying tumor cells use the apoptotic process to generate potent growth-stimulating signals to stimulate the repopulation of tumors undergoing radiotherapy. Furthermore, activated caspase 3, a key executioner in apoptosis, is involved in the growth stimulation. One downstream effector that caspase 3 regulates is prostaglandin E_2 (PGE_2), which can potently stimulate growth of surviving tumor cells. Deficiency of caspase 3 either in tumor cells or in tumor stroma caused substantial tumor sensitivity to radiotherapy in xenograft or mouse tumors. In human subjects with cancer, higher amounts of activated caspase 3 in tumor tissues are correlated with markedly increased rate of recurrence and death. We propose the existence of a cell death–induced tumor repopulation pathway in which caspase 3 has a major role.

There is a large amount of cell death during cytotoxic cancer therapy such as radiation therapy[1,2]. It is normally assumed that dying or dead cells get absorbed by scavenger cells such as macrophages or other surviving cells in the vicinity. The small number of surviving tumor cells, if any, would presumably gradually and slowly proliferate and reestablish the tumor. However, studies that originated more than 40 years ago[3,4] have indicated that tumors respond to radiotherapy by initiating a process called accelerated repopulation. In this process, the few surviving cells that escaped death after exposure to radiotherapy or chemotherapy can rapidly repopulate the badly damaged tumor by proliferating at a markedly accelerated pace. This phenomenon, for which little is understood at the molecular level, has played a major part in modern radiotherapy and chemotherapy[5].

Investigators have made many efforts to understand the molecular mechanism of tumor repopulation after cytotoxic therapy. For example, one study found that radiation-induced upregulation of angiogenesis in tumors was linked with activation of upstream transcriptional factors such as hypoxia-inducible factor-1 (ref. 6). Other recent studies have also indicated the involvement of macrophages in facilitating tumor recovery after radiation[7,8]. Furthermore, one group implicated the integrity of endothelial cells in tumor response to radiotherapy[9]. These reports, although revealing key mechanisms of tumor regrowth, have fallen short of describing the initial driving events responsible for tumor repopulation after radiotherapy.

In this study, we examined the hypothesis that dying cells in the tumor mass may provide the initial signals to promote tumor repopulation. Specifically, we hypothesized that dying cells could release growth-promoting signals to stimulate the proliferation of surviving cells. Our data show a crucial role for intratumoral dying cells in promoting the rapid repopulation of tumors from a small number of live tumor cells. In addition, we made the unexpected discovery that caspase 3, a cysteine protease involved in the 'execution' phase of cellular apoptosis, is a key regulator of growth-promoting signals generated from the dying cells. We believe this newly discovered caspase-mediated tumor repopulation mechanism has key roles in cytotoxic cancer therapy.

RESULTS

Tumor cell repopulation stimulated by cell death *in vitro*

To test our hypothesis, we carried out experiments to examine whether dying tumor cells could stimulate the growth of living tumor cells. To simulate *in vivo* scenarios where the vast majority of tumor cells are killed by radiation or chemotherapy, we seeded a small number (about 500) of firefly luciferase (Fluc)-labeled mouse breast cancer 4T1 cells onto a bed of a much larger number (2.5×10^5) of unlabeled

[1]Experimental Research Center, First People's Hospital, Shanghai Jiao Tong University, Shanghai, China. [2]Department of Radiation Oncology, University of Colorado School of Medicine, Aurora, Colorado, USA. [3]National Laboratory of Oncogenes and Related Genes Research, Cancer Institute, Shanghai Jiao Tong University, Shanghai, China. [4]Department of Radiation Oncology and Ontario Cancer Institute, Princess Margaret Hospital, University of Toronto, Toronto, Ontario, Canada. [5]Department of Environmental and Radiological Health Sciences, Colorado State University, Fort Collins, Colorado, USA. [6]Department of Medicine, University of Colorado School of Medicine, Aurora, Colorado, USA. [7]Department of Surgery, Shanghai First People's Branch Hospital, Shanghai, China. [8]Department of Pathology, University of Colorado School of Medicine, Aurora, Colorado, USA. [9]Head and Neck Cancer Research Program, University of Colorado Cancer Center, Aurora, Colorado, USA. [10]Charles C. Gates Center for Regenerative Medicine and Stem Cell Biology, University of Colorado School of Medicine, Aurora, Colorado, USA. [11]Department of Pharmacology, University of Colorado School of Medicine, Aurora, Colorado, USA. [12]These authors contributed equally to this study. Correspondence should be addressed to C.-Y.L. (chuan.li@ucdenver.edu).

Received 17 November 2009; accepted 27 April 2011; published online 3 July 2011; doi:10.1038/nm.2385

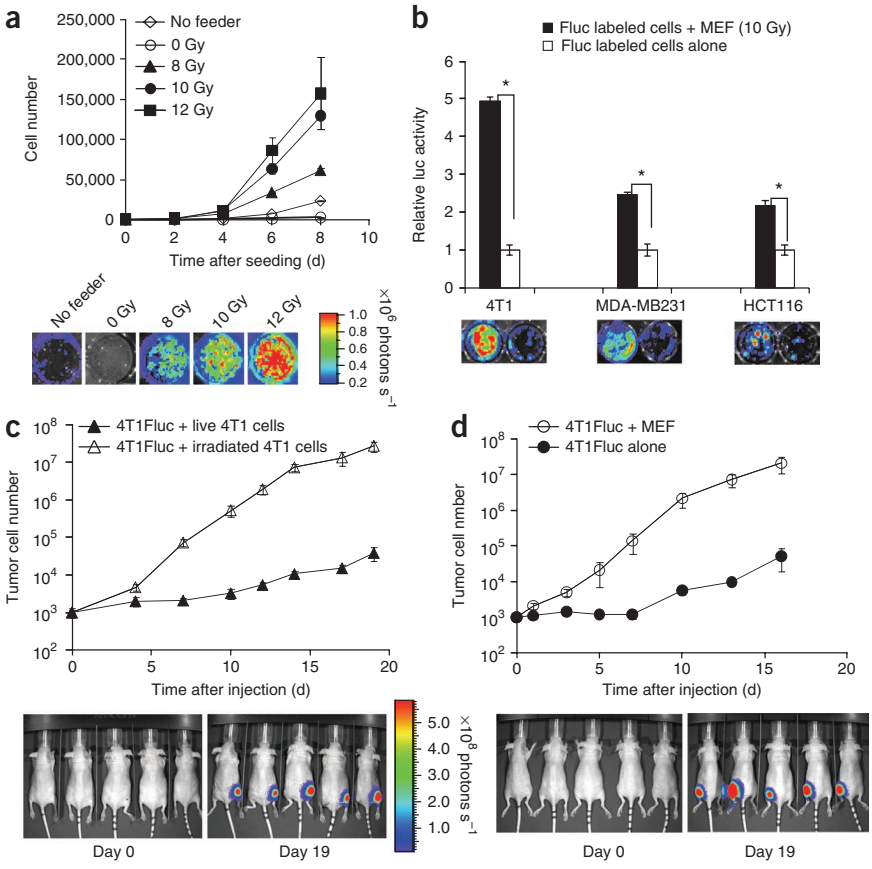

Figure 1 *In vitro* and *in vivo* evidence for the generation of strong growth-stimulating signals in dying cells. (**a**) Stimulation of 4T1Fluc cellular growth *in vitro* by irradiated 4T1 cells. Top, growth of 4T1Fluc cells as observed by luciferase activities. The difference between each of the higher-dose irradiated groups (8, 10 and 12 Gy) and controls (0 Gy and no feeder) was statistically significant ($P < 0.001$, *t* test, $n = 4$). Bottom, representative images from bioluminescence imaging. (**b**) Top, relative growth of MEF-supported tumor cells versus tumor cells seeded alone. $^*P < 0.001$, *t* test, $n = 3$. Bottom, representative bioluminescence images. (**c**,**d**) Effect of dying 4T1 (**c**) and MEF (**d**) cells on 4T1Fluc tumor cellular growth *in vivo*. Top, quantification of bioluminesent signals. Bottom, representative bioluminescent images of mice. In each of the two experiments, the difference between the two groups was highly significant ($P < 0.001$ from day 4 for **c**, and from day 1 for **d**, $n = 5$, one-way analysis of variance (ANOVA) test). In all cases, error bars indicate s.e.m.

'feeder' 4T1 tumor cells that had been irradiated with X-rays at various doses. Growth of the small number of labeled living cells was then monitored through noninvasive bioluminescence imaging[10] (see **Supplementary Fig. 1** for data validating the bioluminescence quantification of tumor cells). Our results indicated that 4T1Fluc cells grew significantly faster when seeded onto dying cells than when seeded alone (**Fig. 1a**). In addition, there was a dose-dependent response from the feeder cells, with non-irradiated feeder cells showing no supportive role and those irradiated with higher radiation doses showing a higher growth-enhancing ability (**Fig. 1a**). Additional supporting evidence came from combinations of other dying versus living cell types, which also showed growth-stimulating properties of dying cells (**Supplementary Figs. 2** and **3**).

Because in solid tumors stromal cells are involved in modulating tumor growth, we also evaluated whether dying fibroblast cells could promote tumor cell growth. Lethally irradiated mouse embryonic fibroblast cells stimulated the growth of various Fluc-labeled tumor cells significantly *in vitro* (**Fig. 1b**).

Tumor cell repopulation stimulated by cell death *in vivo*

We next examined whether cell death–stimulated tumor cell proliferation could be observed *in vivo*. We injected a mix of untreated, Fluc-labeled and lethally irradiated, unlabeled tumor cells (at a ratio of 1:250, or 1,000 live 4T1Fluc cells mixed with 2.5×10^5 unlabeled, lethally irradiated 4T1 cells) subcutaneously into the hind legs of nude mice. Subsequently, we followed the growth of the Fluc-labeled tumor cells over time noninvasively through bioluminescence imaging. As controls, we injected an equal number of Fluc-labeled 4T1 tumor cells mixed with live, unlabeled 4T1 tumor cells into the contralateral hind legs. The presence of lethally irradiated tumor cells markedly increased the growth of Fluc-labeled tumor cells when compared with Fluc-labeled tumor cells injected together with live tumor cells (**Fig. 1c**). In fact the difference in cell numbers, which were derived by dividing total bioluminescent signals by signal intensity of individual cells (**Supplementary Fig. 1**), between the two groups grew exponentially larger and reached as great as 700-fold by the end of the experiment (**Fig. 1c**).

We observed similar *in vivo* tumor growth–promoting properties for mouse embryonic fibroblast (MEF) cells that were irradiated (**Fig. 1d**). Fluc-labeled 4T1 cells co-injected with irradiated fibroblast cells grew to signal intensities 400-fold higher than those from 4T1-Fluc cells injected alone in contralateral hind legs.

Caspase 3 regulates tumor cell repopulation *in vitro*

What is the molecular mechanism for the observed cell death–stimulated proliferation of surviving cells? We reasoned that among the many cellular processes activated or deactivated in dying cells, the factors and processes directly responsible for cell death are most likely to be involved in regulating the growth-promoting properties of dying cells. Therefore, we hypothesized that caspases, the proteases that are involved in both the initiation and the execution of programmed cell death[11], might be involved in regulating the growth-promoting properties of dying cells. To examine this hypothesis, we obtained MEF cells with genetic deletion of the *Casp3* gene[12,13], which encodes the main executioner caspase in mammalian cells, and evaluated the ability of these cells to support the growth of a small number of Fluc-labeled tumor cells. Deficiency in *Casp3* significantly compromised the ability of lethally irradiated MEF cells to stimulate the growth of Fluc-labeled mouse (4T1) and human (MDA-MB231 and HCT116) tumor cells (**Fig. 2a**). The proliferation of Fluc-labeled tumor cells among the irradiated *Casp3*-deficient ($Casp3^{-/-}$) cells reached a degree similar to Fluc-labeled tumor cells seeded alone (**Fig. 2a**), suggesting that caspase 3 was largely responsible for growth stimulation by dying cells.

We confirmed the role of caspase 3 in lethally irradiated 4T1 cells through shRNA-mediated knockdown of *Casp3* expression in feeder cells (**Fig. 2b**) We also confirmed its involvement in the human breast

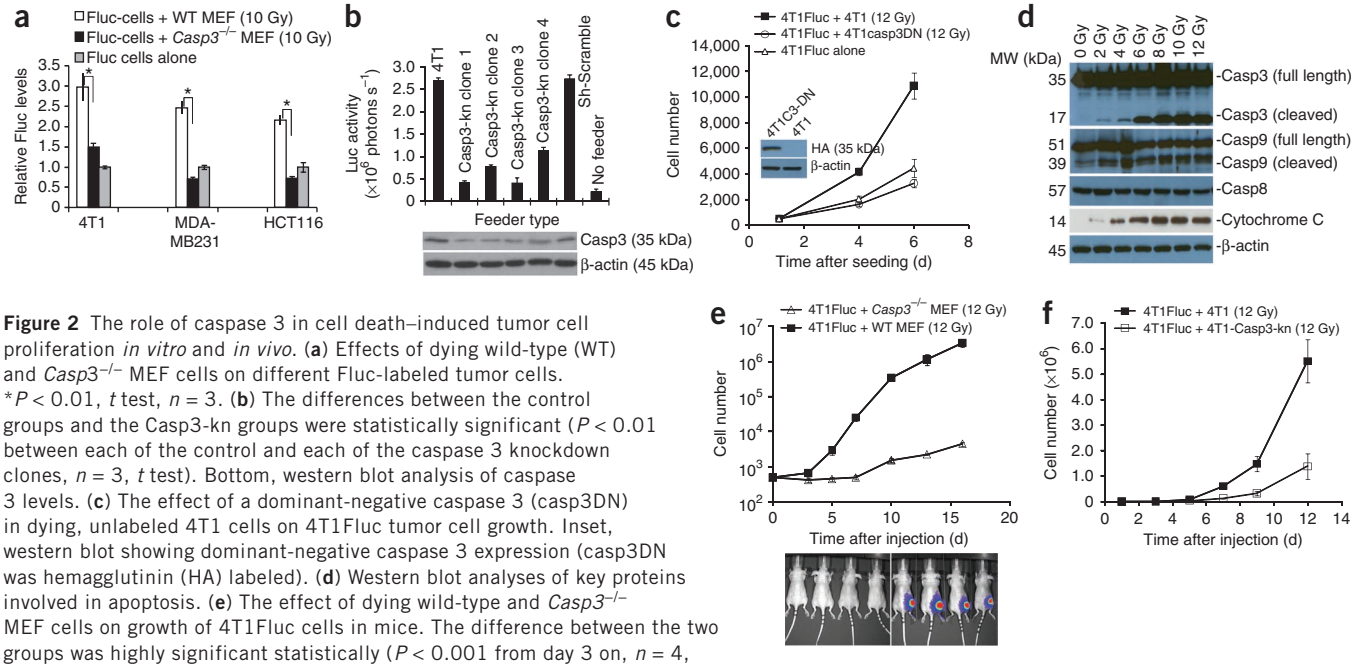

Figure 2 The role of caspase 3 in cell death–induced tumor cell proliferation *in vitro* and *in vivo*. (**a**) Effects of dying wild-type (WT) and *Casp3*$^{-/-}$ MEF cells on different Fluc-labeled tumor cells. $^{*}P < 0.01$, *t* test, $n = 3$. (**b**) The differences between the control groups and the Casp3-kn groups were statistically significant ($P < 0.01$ between each of the control and each of the caspase 3 knockdown clones, $n = 3$, *t* test). Bottom, western blot analysis of caspase 3 levels. (**c**) The effect of a dominant-negative caspase 3 (casp3DN) in dying, unlabeled 4T1 cells on 4T1Fluc tumor cell growth. Inset, western blot showing dominant-negative caspase 3 expression (casp3DN was hemagglutinin (HA) labeled). (**d**) Western blot analyses of key proteins involved in apoptosis. (**e**) The effect of dying wild-type and *Casp3*$^{-/-}$ MEF cells on growth of 4T1Fluc cells in mice. The difference between the two groups was highly significant statistically ($P < 0.001$ from day 3 on, $n = 4$, one-way ANOVA test). (**f**) The effect of caspase 3 knockdown in lethally irradiated 4T1 cells on growth of 4T1Fluc cells *in vivo*. The difference between the two groups was statistically significant from day 5 ($P < 0.05$, $n = 5$, one-way ANOVA test). In all panels, error bars represent s.e.m.

cancer cell line MCF-7, which is deficient in caspase 3 expression. Exogenous expression of caspase 3 significantly increased the ability of lethally irradiated MCF-7 cells to promote the growth of co-seeded MCF-7Fluc cells (**Supplementary Fig. 4**). Because *Casp3*$^{-/-}$ and wild-type MEF cells showed similar clonogenic survival after irradiation (**Supplementary Fig. 5**), we reasoned that the observed defect for *Casp3*$^{-/-}$ MEF cells was not due to the lack of cell death in these cells after radiation. We obtained further data indicating how caspase 3 status markedly affected the modes of cell death in 4T1 (**Supplementary Fig. 6**), MEF (**Supplementary Fig. 7**) and MCF-7 (**Supplementary Fig. 8**) cells after radiation exposure. Our data show that cells could die in multiple ways after radiation exposure. The absence of caspase 3 shifted the mode of cell death from apoptosis to necrosis or autophagy. The **Supplementary Note** contains additional information on these data. To examine whether the proteolytic activity of caspase 3 is required for its role in tumor repopulation, we transduced a dominant-negative version of caspase 3 (C163A)[14] to inhibit caspase 3 cleavage activity in 4T1 cells. 4T1 cells transduced with a gene encoding dominant-negative caspase 3 (C163A)[14] completely lost their ability to support the growth of 4T1Fluc cells (**Fig. 2c**). We obtained similar results by use of a chemical inhibitor of caspase 3, z-VAD-fmk (**Supplementary Fig. 9**).

To confirm that caspase 3 was activated in irradiated cells, we carried out comprehensive immunoblot analyses of various proteins in the apoptotic pathway in irradiated 4T1 (**Fig. 2d**; **Supplementary Table 1** contains antibody information) and MEF (**Supplementary Fig. 10**) cells. Caspases 3 and 9 and the downstream cytochrome *c* were activated in both 4T1 and MEF cells in a dose-dependent manner, whereas caspase 8 was not activated.

Caspase 3 regulation of tumor cell repopulation *in vivo*

To examine the importance of caspase 3 in cell death–stimulated tumor repopulation *in vivo*, we mixed lethally irradiated wild-type or caspase 3–knockout MEF cells with a small number (500) of Fluc-labeled 4T1 cells and injected them subcutaneously into nude mice. In contrast to the potent stimulation of 4T1Fluc tumor cellular growth by lethally irradiated wild-type MEF cells, lethally irradiated caspase 3–deficient MEF cells induced significantly attenuated growth stimulation (**Fig. 2e**). The difference between the two groups was as great as 1,000-fold at later stages of observation (**Fig. 2e**). In fact, in separate experiments, 4T1-Fluc cells injected together with lethally irradiated caspase 3–deficient MEF cells grew at a similar rate to 4T1Fluc cells injected alone in the contralateral legs, indicating a lack of growth stimulation from *Casp3*$^{-/-}$ cells (**Supplementary Fig. 11**).

We also confirmed the role of caspase 3 in regulating growth-promoting properties of dying cells *in vivo* by co-injecting 4T1-Fluc cells with lethally irradiated 4T1 cells transduced with an shRNA minigene targeted against caspase 3. We observed a significant reduction in the ability of lethally irradiated 4T1 cells to stimulate the growth of 4T1-Fluc cells (**Fig. 2f**), consistent with the results obtained with *Casp3*$^{-/-}$ MEF cells.

Growth of injected tumor cells in established tumors

To show that caspase 3 is indeed activated in solid tumors during radiotherapy, we established mouse 4T1 tumor cells transduced with a caspase 3 reporter. Our caspase 3 reporter consists of a luciferase-GFP protein further fused with a polyubiquitin domain (with the whole reporter under the control of a constitutively active cytomegalovirus promoter) that makes the fusion protein susceptible to rapid, proteasome-based degradation. A caspase 3 cleavage site inserted between the polyubitquitin domain and the luciferase-GFP domain ensures that the reporter is stabilized and detectable when caspase 3 is activated (**Fig. 3a**, left). **Supplementary Figure 12** shows data supporting the functionality of our caspase 3 reporter. We established tumors from reporter-containing cells and irradiated them with X-rays (6 Gy) when they reached 5–7 mm in diameter. We then observed caspase 3 activation in the tumors through quantitative bioluminescence imaging. Our results showed that caspase 3 was significantly activated (as much as 30-fold at its peak when compared with that of nonirradiated control tumors) at days 3, 5 and 7 after radiotherapy (**Fig. 3a**).

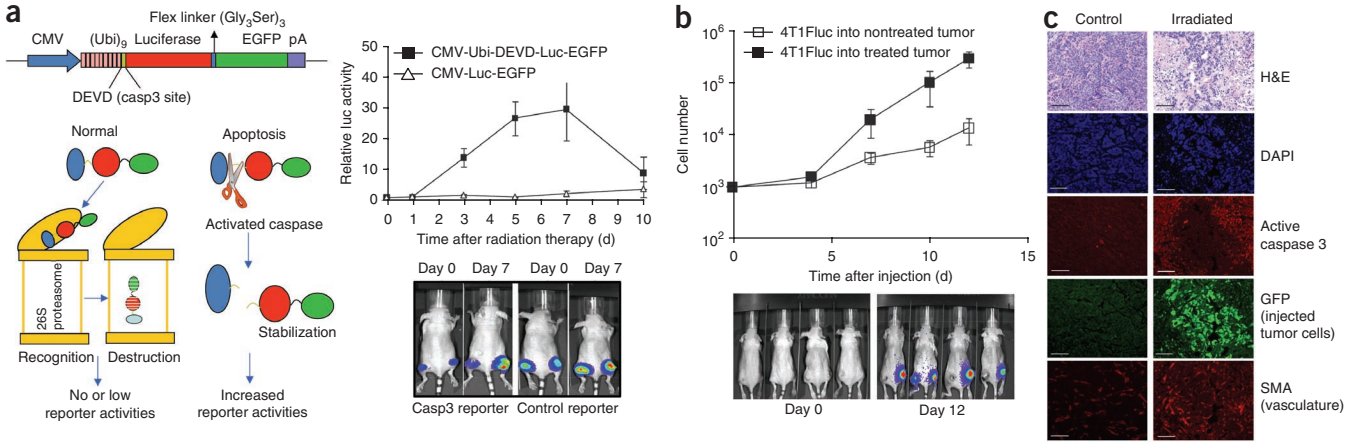

Figure 3 Relationship between caspase activation and growth of injected tumor cells in the irradiated tumor microenvironment. (**a**) Caspase 3 activation in 4T1 tumors as detected by a caspase 3 reporter. Left, schematic of the structure of a proteasome-based caspase 3 reporter (top left) and its mode of action (bottom left). Right, caspase 3 activities in 4T1 tumors transduced with the control as well as *Casp3* reporter genes. The difference between the control and caspase 3 reporter groups are significant at days 3, 5 and 7 ($P < 0.01$, $n = 5$, t test). CMV, cytomegalovirus promoter; $(Ubi)_9$, polyubiqutin domain consists of nine tandem copies of ubiquitin; pA, polyadenylation signal; DEVD, consensus caspase 3 cleavage site. (**b**) Top, growth of 4T1Fluc cells injected into irradiated and nonirradiated established tumors. The difference between the two groups was statistically significant ($P < 0.05$ from day 7, t test, $n = 4$). Bottom, representative images of tumor-bearing mice. (**c**) Immunofluorescence analysis of growth of intratumorally injected GFP-labeled cells and the indicated protein expression surrounding the injected cells. SMA, smooth muscle actin, a marker for blood vessels. Scale bars, 100 μm. Error bars represent s.e.m.

In another experiment, we injected a small number of Fluc-labeled 4T1 tumor cells (about 1,000) into previously nonirradiated and irradiated 4T1 tumors established from unlabeled cells in the left and rights sides of host mice, respectively. We then observed the growth of labeled tumor cells through bioluminescence imaging. Cells injected into irradiated tumors grew at a significantly faster rate than those injected into nontreated tumors (**Fig. 3b**), consistent with earlier results.

In a further experiment, we injected 4T1 cells stably transduced with GFP into irradiated tumors and allowed them to grow for 5–8 d. We then killed the mice, excised the tumors and examined them for expression of various proteins. There was a clear relationship between activated caspase 3 and the proliferation of injected, GFP-labeled tumor cells in irradiated tumor cells, as indicated by the complementary patterns of caspase 3 staining and injected tumor cell staining (**Fig. 3c**). In contrast, we observed very little injected tumor cell growth and caspase activation in non-irradiated tumors (**Fig. 3c**). In addition to caspase activation, irradiated tumors also showed increased, localized neovasculature, as determined by SMA staining (**Fig. 3c**). Irradiated tumors also showed a significant influx of macrophages (**Supplementary Fig. 13**), which have been shown to stimulate tumor angiogenesis and tumor growth.

A downstream target for caspase 3 in tumor repopulation

We next attempted to identify the downstream factors of caspase 3 that were involved in generating growth-promoting factors from the dying cells. We focused on cytosolic calcium-independent phospholipase A_2, group 6 ($iPLA_2$, encoded by *PLA2G6*), because it had previously been reported that its phosopholipase activity was activated by caspase 3 cleavage[15–17]. Earlier reports have shown that caspase 3-mediated $iPLA_2$ (Pla2g6) activation led to increased production of arachidonic acid[15], whose downstream eicosanoid derivatives (such as PGE_2) had been implicated in stimulating tumor growth[18] and stem cell proliferation[19]. To evaluate the potential involvement of the caspase-activated $iPLA_2$–arachidonic acid–PGE_2 axis in cell death–induced tumor cell proliferation, we transduced shRNA targeting *Pla2g6* into 4T1 tumor cells or wild-type MEF cells and examined whether these cells, when lethally irradiated, could support Fluc-labeled

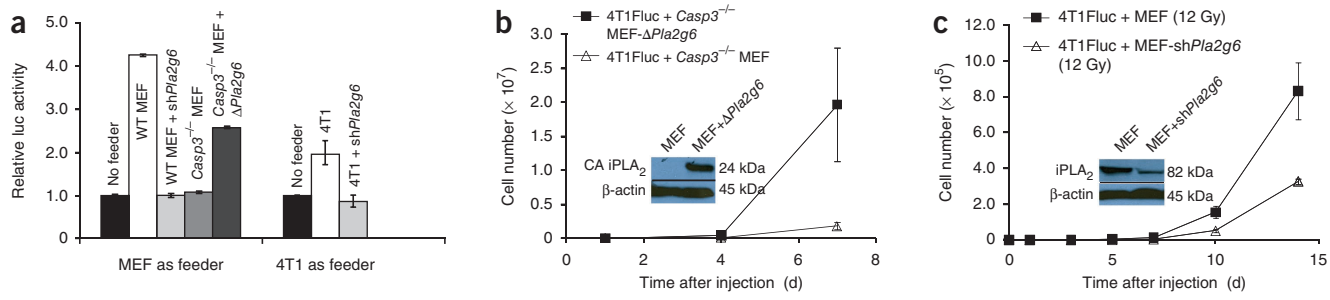

Figure 4 A role for caspase 3–activated $iPLA_2$ (*Pla2g6*) in facilitating cell death–stimulated tumor cell repopulation. (**a**) The effect of *Pla2g6* levels in dying cells on the growth of 4T1Fluc cells *in vitro*. $P < 0.01$, $n = 4$, t test. (**b**) The effect of constitutively active (CA) $iPLA_2$ Δ*Pla2g6* in $Casp3^{-/-}$ MEF cells *in vivo*. The differences between the luciferase signals were statistically significant ($P < 0.01$ on day 7, $n = 5$, t test). Inset, expression of truncated $iPLA_2$. (**c**) The *in vivo* effect of $iPLA_2$ knockdown in wild-type MEF cells. The difference between the two groups was statistically significant from day 3 ($P < 0.02$, from day 7, $n = 5$, one-way ANOVA). Inset, western blot analysis of shRNA knockdown of *Pla2g6*. Error bars represent s.e.m.

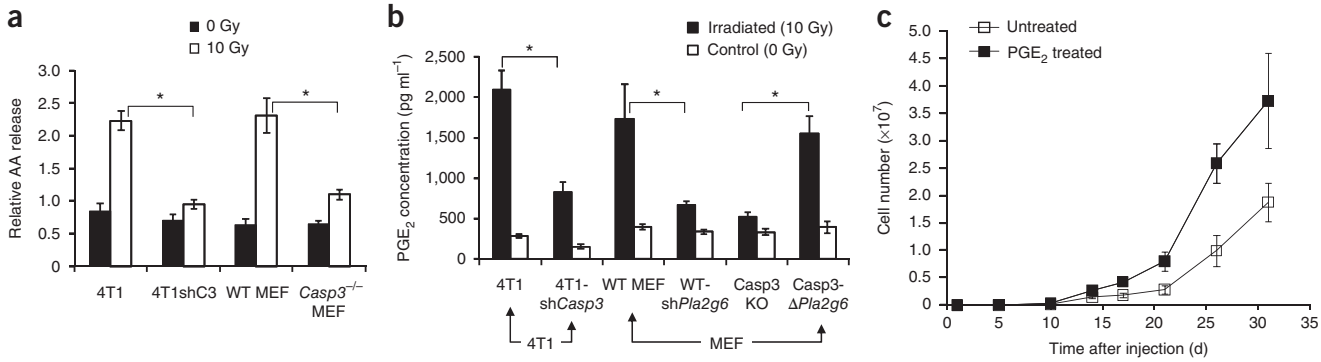

Figure 5 Regulation of radiation-induced arachidonic acid release and PGE_2 production by caspase 3. (**a**) Arachidonic acid (AA) release. $*P < 0.02$ (*t* test, $n = 3$). (**b**) PGE_2 secretion. $*P < 0.05$ (*t* test, $n = 3$). (**c**) PGE_2-stimulated tumor growth from 1,000 4T1Fluc tumor cells injected subcutaneously into nude mice. The difference between the two groups are statistical significant from day 17 ($P < 0.05$, $n = 5$, one-way ANOVA). Error bars represent s.e.m.

tumor cell growth to the same extent as their wild-type untreated counterparts. In both MEF and 4T1 cells, expression of shRNA against *Pla2g6* significantly reduced the ability of these cells to stimulate Fluc-labeled 4T1 cellular proliferation after irradiation (**Fig. 4a**). Western blot analysis also indicated that $iPLA_2$ is indeed activated in a caspase 3–dependent manner (**Supplementary Fig. 14**) in both 4T1 and MEF cells. These results are consistent with multiple earlier reports[15–17].

We next transduced a truncated version of the *Pla2g6* gene (Δ*Pla2g6*), which encodes an $iPLA_2$ fragment (containing the catalytic domain) that is a predicted product of caspase 3 cleavage of $iPLA_2$, into caspase 3–deficient MEF cells. After Δ*Pla2g6* transduction (inset of **Fig. 4a**), lethally irradiated *Casp3*$^{-/-}$ cells were significantly better at stimulating the growth of Fluc-labeled 4T1-Fluc cells both *in vitro* (**Fig. 4a**) and *in vivo* (**Fig. 4b** and **Supplementary Fig. 15**) when compared with parental *Casp3*$^{-/-}$ cells.

Knocking down *Pla2g6* gene expression (**Fig. 4c**) significantly reduced the ability of lethally irradiated MEF cells to stimulate the growth of 4T1-Fluc cells *in vivo* (**Fig. 4c** and **Supplementary Fig. 16**). In established wild-type or *Pla2g6* knockdown 4T1 tumors, growth of subsequently transplanted 4T1Fluc cells was significantly slowed (**Supplementary Fig. 17**).

Caspase 3, $iPLA_2$ activation and PGE_2 release

Because arachidonic acid is one of two main catalytic products of activated $iPLA_2$ (the other being lysophosphatidic choline), we measured radiation-induced release of arachidonic acid into the extracellular milieu to examine the potential relationship between caspase 3 and arachidonic acid release. We found that irradiation of wild type MEF cells stimulated the release of arachidonic acid into the supernatant (**Fig. 5a**). However, this release was substantially reduced in *Casp3*$^{-/-}$ MEF cells, indicating a crucial role for caspase 3. In addition, arachidonic acid release was also markedly reduced in 4T1 cells with knockdown of *Casp3* gene expression (**Fig. 5a**).

Because PGE_2, a key regulator of tumor growth, is a downstream product of arachidonic acid, we measured PGE_2 production induced by ionizing radiation in the supernatants of cells. Exposure to ionizing radiation markedly induced the production of PGE_2 in wild-type MEF cells as well as in 4T1 tumor cells when compared with nonirradiated cells (**Fig. 5b**). However, in *Casp3*$^{-/-}$ MEF cells and in 4T1sh*Casp3* cells, the production of PGE_2 in irradiated cells was considerably reduced compared with wild-type cells (**Fig. 5b**). In contrast, transduction of a constitutively active, truncated *Pla2g6* (**Fig. 4b**, inset) (which encodes a protein that is equivalent to a caspase-cleaved version of $iPLA_2$), substantially restored PGE_2 production in *Casp3*$^{-/-}$ MEF cells (**Fig. 5b**). In an additional experiment, cyclooxygenase 2 and its upstream transcription factor nuclear factor-κB, which have crucial roles in PGE_2 production, were shown to be activated in a caspase 3–independent manner (**Supplementary Fig. 18**). Consistent with this, indomethacin (a cyclooxygenase 1 and 2 inhibitor) administration effectively suppressed growth of intratumorally injected 4T1 and HCT116 cells (**Supplementary Fig. 19**).

Treatment of a small number (1,000) of tumor cells with PGE_2 gave the treated cells a significant head start, allowing them to grow at a faster pace than untreated cells when injected into mice (**Fig. 5c**). In contrast, shRNA-mediated downregulation of EP_2, a receptor for PGE_2, in 4T1Fluc cells markedly attenuated the proliferation of the latter when seeded together with lethally irradiated 4T1 cells (**Supplementary Fig. 20**).

Caspase 3 and radiosensitivities of tumors in mice and man

To examine the prospect of enhancing cancer radiotherapy through inhibition of caspase 3, we carried out two experiments in mouse tumor models. In the first experiment, we used MCF-7 cells, which are naturally deficient in caspase 3 expression (**Supplementary Fig. 8**). We established tumor xenografts in female nude mice using both parental MCF-7 cells and a modified MCF-7 cell line with an exogenously transduced copy of the gene encoding human caspase 3 (*CASP3*). The transduction of *CASP3* into MCF-7 cells rendered them significantly more susceptible to apoptosis (**Supplementary Fig. 8**). Unexpectedly, *CASP3* transduction also enabled MCF-7 cells to form tumors at a faster pace in the absence of radiotherapy. Although we do not fully understand the mechanism for this observation, we speculate that cell death is common during tumor growth, and growth-promoting signals from the dying cells may have a role in regulating overall tumor growth even in the absence of cytotoxic treatments (**Fig. 6a**). Notably, the presence of caspase 3 made MCF-7 *CASP3* tumors significantly more resistant to radiotherapy than parental MCF-7 tumors, which disappeared completely after two doses of 6 Gy X-rays and did not regrow during the entire course of observation (**Fig. 6a**). In contrast, tumors established from MCF-7 *CASP3* cells kept growing after irradiation despite growing more slowly than control, nonirradiated tumors (**Fig. 6a**). Because MCF-7 *CASP3* cells showed substantially more and faster radiation-induced apoptototic cell death *in vitro* (**Supplementary Fig. 8**), our results are consistent with the interpretation that MCF-7*CASP3* tumors showed more resistance to radiation as a result of faster tumor cell repopulation instead of intrinsic resistance, although we could not

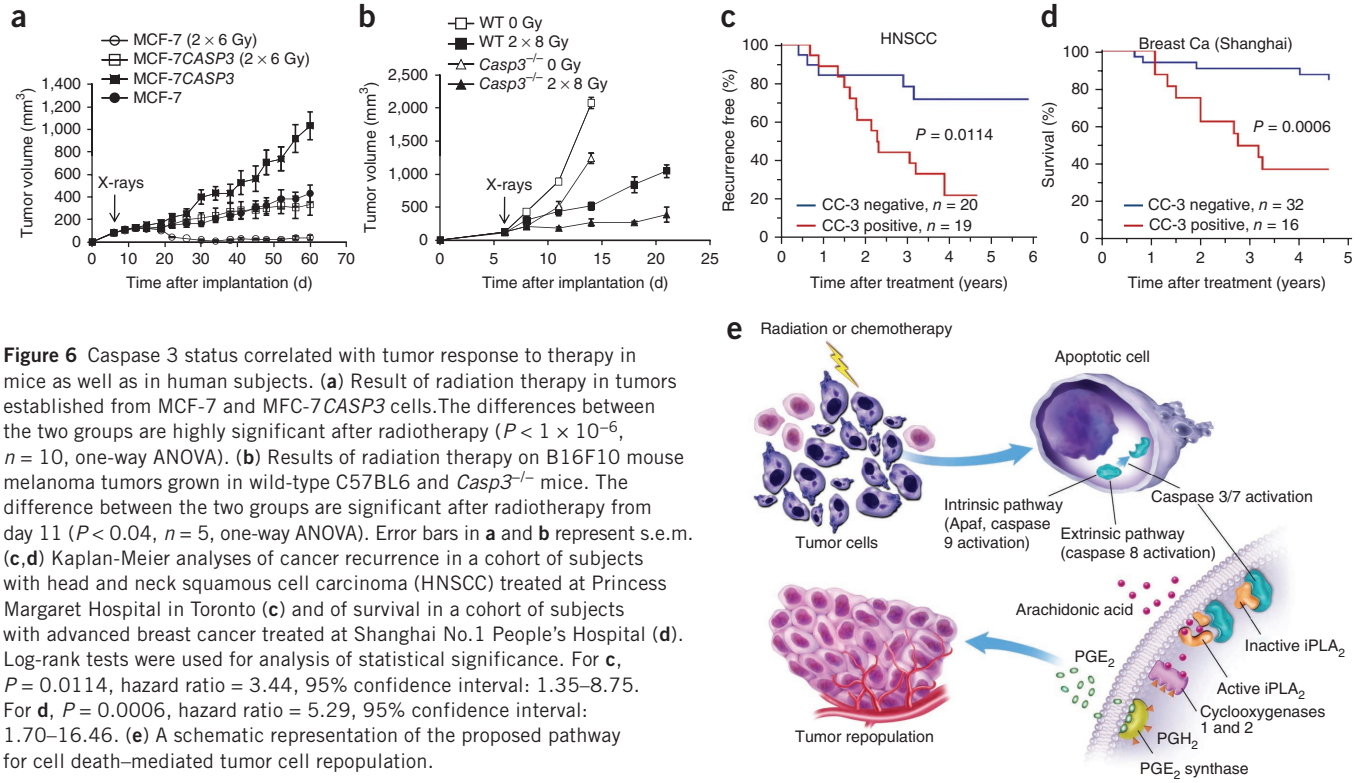

Figure 6 Caspase 3 status correlated with tumor response to therapy in mice as well as in human subjects. (**a**) Result of radiation therapy in tumors established from MCF-7 and MFC-7*CASP3* cells.The differences between the two groups are highly significant after radiotherapy ($P < 1 \times 10^{-6}$, $n = 10$, one-way ANOVA). (**b**) Results of radiation therapy on B16F10 mouse melanoma tumors grown in wild-type C57BL6 and *Casp3*$^{-/-}$ mice. The difference between the two groups are significant after radiotherapy from day 11 ($P < 0.04$, $n = 5$, one-way ANOVA). Error bars in **a** and **b** represent s.e.m. (**c**,**d**) Kaplan-Meier analyses of cancer recurrence in a cohort of subjects with head and neck squamous cell carcinoma (HNSCC) treated at Princess Margaret Hospital in Toronto (**c**) and of survival in a cohort of subjects with advanced breast cancer treated at Shanghai No.1 People's Hospital (**d**). Log-rank tests were used for analysis of statistical significance. For **c**, $P = 0.0114$, hazard ratio = 3.44, 95% confidence interval: 1.35–8.75. For **d**, $P = 0.0006$, hazard ratio = 5.29, 95% confidence interval: 1.70–16.46. (**e**) A schematic representation of the proposed pathway for cell death–mediated tumor cell repopulation.

rule out additional mechanisms such as enhanced tumor angiogenesis due to caspase 3–mediated PGE_2 production.

In the second experiment, we attempted to examine the potential role of stroma-derived caspase 3 activities in tumor response to radiotherapy, because stroma accounts for a substantial percentage of tumor mass. We established tumors in wild-type as well as *Casp3*$^{-/-}$ mice with B16F10 cells, which is a metastatic and radioresistant tumor line syngeneic with the C57BL/6 mice. We carried out radiotherapy (two doses of 8 Gy) when tumors reached 5–7 mm in diameter. B16F10 tumors grown in *Casp3*$^{-/-}$ mice showed significant sensitivity to radiotherapy when compared with those in wild-type C57BL/6 mice (**Fig. 6b**). Our results therefore confirm the role of caspase 3 in both tumor cells and tumor stroma in stimulating tumor response to radiotherapy.

To determine the relevance of caspase-mediated tumor repopulation in human cancer treatment, we evaluated caspase 3 status in two cohorts of human subjects with cancer. In the first cohort, 39 subjects with head and neck cancer treated with radiotherapy or chemo-radiotherapy at the Princess Margaret Hospital in Toronto (see **Supplementary Table 2** for subject characteristics) were examined for activated caspase 3 through immunohistochemical analysis of pretreatment tumor biopsies. Consistent with our results in mice (**Fig. 6a**,**b**), subjects with high (>10% staining) amounts of cleaved (and thus activated) caspase 3 in their tumor samples showed a significantly ($P = 0.011$) higher rate of tumor recurrence (**Fig. 6c** and **Supplementary Fig. 21**). In the second cohort, 48 subjects with advanced stage breast cancer treated at Shanghai No. 1 People's hospital (see **Supplementary Table 3** for subject characteristics) were analyzed for activated caspase 3 expression through immunohistochemical analysis of pretreatment biopsies. Subjects with strong cleaved caspase 3 staining (>10% cells stained) had significantly ($P = 0.0002$) shorter survival times (**Fig. 6d** and **Supplementary Fig. 22**). The mechanism by which caspase 3 is activated in pretreatment biopsies remains unknown. In addition, we analyzed public domain microarray data from a previously published study[20]. In 249 subjects with breast cancer from Sweden and Singapore, elevated caspase 3 mRNA levels correlated with significantly elevated risk ($P = 0.0001$) of relapse (**Supplementary Fig. 23**). On the basis of our results, we conclude that elevated tumor caspase 3 levels predict worse treatment outcomes in people with cancer.

We propose the existence of a cell death-mediated tumor repopulation pathway in which caspase 3 plays a major role (**Fig. 6e**).

DISCUSSION

In tumors exposed to cytotoxic cancer therapeutics, cells live and die depending on the extent of damage they have suffered. In this study, we have provided evidence that these two types of cells are inextricably associated, manifested by our observation that apoptotic tumor cells stimulate the repopulation of tumors from a small number of surviving cells. Caspase 3, the master executioner during apoptotic cell death, serves as a direct link between cell death and tumor repopulation. Despite the paradoxical nature of these results at first glance, however, we believe the observed link between cellular death and proliferation may be one of the key mechanisms of metazoan tissue homeostasis exploited by tumors to preserve themselves when damaged by cytotoxic treatments. Indeed, the phenomenon of apoptosis-stimulated tissue regeneration has been observed by other investigators in lower organisms such as *Drosophila* and hydra systems[21–23]. In these cases, it has been proposed that apoptotic cells stimulate so-called compensatory proliferation for tissue regeneration. The mechanisms involved are not entirely clear. However, it was reported that β-catenin–Wnt signaling was involved in some instances of compensatory proliferation[23]. In this context, it is notable that PGE_2 has been shown to activate the β-catenin–Wnt signaling pathway in colon cancer[18]. Therefore, the caspase-$iPLA_2$ pathway that we unveiled here may be part of the evolutionarily conserved mechanism for tissue repair.

Although a direct role for caspase 3 in stimulating tumor repopulation has not been described before to our knowledge, there have been many published studies on nonapoptotic roles of caspases in mammalian biology. Examples of these include caspase-mediated stimulation of differentiation[24–26], dedifferentiation[27] and T cell activation[28]. Other possible caspase 3–mediated effects include how the host immune system will be mobilized against cancer cells, which can be heavily influenced by how cells die (for example, necrosis versus apoptosis).

One of the practical implications of this study is a new and counter-intuitive approach to enhancing cancer radiotherapy through caspase 3 inhibition. Our results point to the potential efficacy of adjuvant use of caspase 3 inhibitors in radiotherapy. Another implication of our study is the potential use of activated caspase 3 as a biomarker to predict tumor response to treatment, as supported by data from immunohistochemical analyses of human tumor samples.

Finally, we believe our newly discovered, caspase 3–regulated tumor repopulation pathway has profound implications for the understanding of cancer biology and treatment. It also provides an example of how tumor cells usurp a key metazoan tissue regeneration mechanism[29] for their own survival.

METHODS

Methods and any associated references are available in the online version of the paper at http://www.nature.com/naturemedicine/.

Note: Supplementary information is available on the Nature Medicine website.

ACKNOWLEDGMENTS

We thank R. Flavell of Yale University for providing us with MEF cells with caspase 3 or 7 deficiencies. We thank B. Liu of University of Colorado School of Medicine for providing us with the MCF-7 and MCF-7*CASP3* cells. We also thank P. Kabos for insightful discussions. This study was supported in part by grants CA131408 and CA136748 from the US National Cancer Institute (to C.-Y.L.), and grant NNX09AH19G (to C.-Y.L.) from US National Aeronautics and Space Administration Ground-based Space Radiation Biology Research Program. It was also supported by a subcontract (to C.-Y.L.) of grant DEFG0207ER64350 (to J.S.B.) from the US Department of Energy Low Dose Radiation Research Program. Q.H. was supported by grant 2010CB529900 from the National Basic Research Project of China and Outstanding Young Scientist grants 30325043 & 30428015 from China National Natural Science Foundation.

AUTHOR CONTRIBUTIONS

Q.H. and F.L. designed and conducted most of the experiments, analyzed data and wrote the manuscript. X.L. and W.L. carried out analyses on modes of cell death in irradiated cells; W.S. carried out immunohistochemical analysis of human head and neck tumor samples; F.-F.L. and B.O. provided human head and neck cancer samples and analyzed data from the samples; Z.H. conducted some of the caspase reporter experiments; Y.P. carried out arachidonic acid release experiments and J.S.B. analyzed relevant data of arachidonic acid release; A.-C.T. carried out data analyses of human clinical data; G.H. and X.-J.W. helped with immunohistochemical analysis of mouse tumor samples; J.S. constructed some of the plasmids used; A.J. and D.R. provided human head and neck tumor samples; L.Z. carried out immunohistochemical analysis of human breast cancer samples; J.T. and A.T. helped to conduct experiments on autophagy and necrosis; C.-Y.L. conceived of the study, analyzed data and wrote the manuscript. All authors read and agreed on the final manuscript.

COMPETING FINANCIAL INTERESTS

The authors declare no competing financial interests.

Published online at http://www.nature.com/naturemedicine/.
Reprints and permissions information is available online at http://www.nature.com/reprints/index.html.

1. Steel, G.G. Cell survival as a determinant of tumor response in *Basic Clinical Radiobiology* (ed. Steel, G.G.) 52–63 (Hodder Arnold, London, 2002).
2. Gilewski, T. & Norton, L. Cytokinetics. in *Cancer Medicine* (eds. Kufe, D. *et al.*) 570–589 (BC Decker, Hamilton, London, 2006).
3. Hermens, A.F. & Barendsen, G.W. Changes of cell proliferation characteristics in a rat rhabdomyosarcoma before and after x-irradiation. *Eur. J. Cancer* **5**, 173–189 (1969).
4. Stephens, T.C., Currie, G.A. & Peacock, J.H. Repopulation of gamma-irradiated Lewis lung carcinoma by malignant cells and host macrophage progenitors. *Br. J. Cancer* **38**, 573–582 (1978).
5. Hall, E. & Giaccia, A. *Radiobiology for the Radiologist* 378–397 (Lippincott Williams & Wilkins, Philadelphia, 2006).
6. Moeller, B.J., Cao, Y., Li, C.Y. & Dewhirst, M.W. Radiation activates HIF-1 to regulate vascular radiosensitivity in tumors: role of reoxygenation, free radicals and stress granules. *Cancer Cell* **5**, 429–441 (2004).
7. Li, F. *et al.* Regulation of HIF-1alpha stability through S-nitrosylation. *Mol. Cell* **26**, 63–74 (2007).
8. Ahn, G.O. & Brown, J.M. Matrix metalloproteinase-9 is required for tumor vasculogenesis but not for angiogenesis: role of bone marrow–derived myelomonocytic cells. *Cancer Cell* **13**, 193–205 (2008).
9. Garcia-Barros, M. *et al.* Tumor response to radiotherapy regulated by endothelial cell apoptosis. *Science* **300**, 1155–1159 (2003).
10. Contag, C.H., Jenkins, D., Contag, P.R. & Negrin, R.S. Use of reporter genes for optical measurements of neoplastic disease *in vivo*. *Neoplasia* **2**, 41–52 (2000).
11. Taylor, R.C., Cullen, S.P. & Martin, S.J. Apoptosis: controlled demolition at the cellular level. *Nat. Rev. Mol. Cell Biol.* **9**, 231–241 (2008).
12. Kuida, K. *et al.* Decreased apoptosis in the brain and premature lethality in CPP32-deficient mice. *Nature* **384**, 368–372 (1996).
13. Lakhani, S.A. *et al.* Caspases 3 and 7: key mediators of mitochondrial events of apoptosis. *Science* **311**, 847–851 (2006).
14. Stennicke, H.R. & Salvesen, G.S. Biochemical characteristics of caspases-3, -6, -7 and -8. *J. Biol. Chem.* **272**, 25719–25723 (1997).
15. Atsumi, G. *et al.* Fas-induced arachidonic acid release is mediated by Ca^{2+}-independent phospholipase A2 but not cytosolic phospholipase A2, which undergoes proteolytic inactivation. *J. Biol. Chem.* **273**, 13870–13877 (1998).
16. Lauber, K. *et al.* Apoptotic cells induce migration of phagocytes via caspase-3-mediated release of a lipid attraction signal. *Cell* **113**, 717–730 (2003).
17. Zhao, X. *et al.* Caspase-3–dependent activation of calcium-independent phospholipase A2 enhances cell migration in non-apoptotic ovarian cancer cells. *J. Biol. Chem.* **281**, 29357–29368 (2006).
18. Castellone, M.D., Teramoto, H., Williams, B.O., Druey, K.M. & Gutkind, J.S. Prostaglandin E_2 promotes colon cancer cell growth through a G_s-axin-β-catenin signaling axis. *Science* **310**, 1504–1510 (2005).
19. North, T.E. *et al.* Prostaglandin E_2 regulates vertebrate haematopoietic stem cell homeostasis. *Nature* **447**, 1007–1011 (2007).
20. Ivshina, A.V. *et al.* Genetic reclassification of histologic grade delineates new clinical subtypes of breast cancer. *Cancer Res.* **66**, 10292–10301 (2006).
21. Ryoo, H.D., Gorenc, T. & Steller, H. Apoptotic cells can induce compensatory cell proliferation through the JNK and the Wingless signaling pathways. *Dev. Cell* **7**, 491–501 (2004).
22. Fan, Y. & Bergmann, A. Distinct mechanisms of apoptosis-induced compensatory proliferation in proliferating and differentiating tissues in the *Drosophila* eye. *Dev. Cell* **14**, 399–410 (2008).
23. Chera, S. *et al.* Apoptotic cells provide an unexpected source of Wnt3 signaling to drive hydra head regeneration. *Dev. Cell* **17**, 279–289 (2009).
24. Kang, T.B. *et al.* Caspase-8 serves both apoptotic and nonapoptotic roles. *J. Immunol.* **173**, 2976–2984 (2004).
25. Szymczyk, K.H., Freeman, T.A., Adams, C.S., Srinivas, V. & Steinbeck, M.J. Active caspase-3 is required for osteoclast differentiation. *J. Cell. Physiol.* **209**, 836–844 (2006).
26. Fujita, J. *et al.* Caspase activity mediates the differentiation of embryonic stem cells. *Cell Stem Cell* **2**, 595–601 (2008).
27. Li, F. *et al.* Apoptotic caspases regulate induction of iPSCs from human fibroblasts. *Cell Stem Cell* **7**, 508–520 (2010).
28. Kennedy, N.J., Kataoka, T., Tschopp, J. & Budd, R.C. Caspase activation is required for T cell proliferation. *J. Exp. Med.* **190**, 1891–1896 (1999).
29. Li, F. *et al.* Apoptotic cells activate the "phoenix rising" pathway to promote wound healing and tissue regeneration. *Sci. Signal.* **3**, ra13 (2010).

ONLINE METHODS

Cells and tissue culture conditions. We used a variety of cancer and fibroblast cells in this study. Among these are the mouse breast cancer cell line 4T1, mouse fibroblast cell lines NIH3T3, human cancer cell lines MCF-7 (breast cancer line), MDA-MB231 (breast cancer line), HCT116 (colon cancer line) and human fibroblast cell strain IMR-90. Additional details are in the **Supplementary Methods**.

Bioluminescence imaging. For imaging luciferase, we used the IVIS200 instrument from Caliper Life Sciences. For tissue-cultured cells, we imaged luciferase signal by adding PBS or colorless OptiMEM medium (Invitrogen) with D-luciferin (Caliper Life Sciences) at a concentration of 0.15 mg ml^{-1}. Cells were imaged 10 min after luciferin administration. After images were taken, we used manufacturer-supplied software to process the images for quantitative data.

To monitor growth of Fluc-labeled cells *in vitro*, about 500 or 1,000 cells were mixed together with an overwhelming number of (for example 2×10^5) unlabeled cells either right after irradiation or 24 h after irradiation (or other cytotoxic treatments). The cells were then monitored at different times for up to 8 d after seeding by use of IVIS200.

Growth of Fluc-labeled tumor cells *in vivo* was followed through noninvasive bioluminescence imaging using the IVIS200 instrument (Caliper Life Sciences). Mice to be imaged were injected with 150 mg per kg body weight of D-luciferin intraperitoneally in 200 µl of PBS and then anesthetized with continuous flow of isofluorane. Imaging of the mice was carried out 10 min later.

Monitoring tumor cell growth in mice. We used different approaches to establish tumor growth than those traditionally adopted by other studies. In most of our studies, we injected a very small number of Fluc-labeled tumor cells (500–1,000 cells each) either alone or together with other unlabeled cells (either tumor cells or fibroblast cells) that were either irradiated or not irradiated. Tumor growth from these cells was monitored through the quantification of bioluminescence signals emitted from labeled tumor cells by use of the IVIS200 instrument following the manufacturer's instructions. In some cases, 500–1,000 Fluc-labeled tumor cells were injected into tumors (7–9 mm in diameter) that had been established from unlabeled tumor cells.

Tumor growth delay experiments. To evaluate the function of caspase 3 in tumor radiotherapy, about 3×10^6 MCF-7 and MCF-7*CASP3* tumor cells were injected subcutaneously with Matrigel and established in female nude mice implanted with estrogen pellets (1.7 mg per pellet, 60-d release formula, Innovative Research of American). When tumors reached 5–7 mm in diameter, they were exposed to X-ray irradiation (two doses of 6 Gy). The sizes of the tumors were measured every other day with a caliper. In separate experiments, B16F10 melanoma cells were injected into syngeneic C57BL/6 wild-type and caspase 3–knockout mice (Jackson Laboratory), and tumor growth experiments were conducted when tumors reached 5–7 mm in diameter.

Mouse experiments. Animal experimental procedures were approved by the University of Colorado Denver Institutional Animal Care and Use Committee.

Human tumor samples. Clinical human tumor samples were acquired with informed consent following protocols approved by University Health Network Research Ethics Board (for samples from Princess Margaret Hospital samples) and Committee on Research Ethics (for samples from Shanghai First People's Hospital), respectively.

Additional methods. Detailed methodology is described in the **Supplementary Methods**.